

# A Low Phase Error Vector Modulator Using TEST Tunable I/Q Generator for mmWave Communication

Jinhyun Kim<sup>1</sup>, Graduate Student Member, IEEE, Seongwoog Oh<sup>1</sup>, Graduate Student Member, IEEE, and Jungsuek Oh<sup>1</sup>, Senior Member, IEEE

**Abstract**—This letter presents a low phase error with a high gain vector modulator in a 28 nm CMOS process. It consists of an input balun network (IBN), a tunable I/Q generator, a variable gain amplifier (VGA), and an output balun network (OBN). The proposed I/Q generator uses two transformer-based couplers and a varactor. Through the control of the varactor, the I/Q generator can optimize the operation frequency at which the phase difference of each quadrature signal is 90°. To implement the proposed I/Q generator, the IBN uses a cascode topology to isolate between the IBN and I/Q generator. The proposed vector modulator achieved a phase shift of 22.5° and had an average root-mean-square (rms) phase error of 2.89° and an rms gain error of 1.57 dB at the 31–36 GHz band. The maximum average gain was −3.48 dB at 33 GHz, and the power consumption was 28.8 mW from a 1.8 V supply. The proposed vector modulator achieved a high gain with a low rms phase error based on the tunable I/Q generator in the *Ka*-band.

**Index Terms**—Millimeter wave, monolithic microwave integrated circuit, phase shifter, tunable I/Q generator, vector modulator.

## I. INTRODUCTION

IN RECENT years, the demand for mmWave systems has been rapidly growing for 5G and satellite communications. In particular, because the path loss is large in the mmWave band, communication based on a phased array antenna capable of achieving beam forming and beam steering is essential. Accordingly, a high-performance phase shifter is required to control phased array antennas [1], [2], [3], [4].

To implement a high-quality phase shifter, the design parameters such as gain, phase error, phase resolution, and low power consumption are required to design the phase shifter. Therefore, considerable research has been conducted on passive type

Manuscript received 8 February 2023; accepted 19 April 2023. Date of publication 8 May 2023; date of current version 7 July 2023. This work was supported in part by the Institute of Information and Communications Technology Planning and Evaluation (IITP) Grant Funded by the Korean government (MSIT) under Grant 2021-0-00763; in part by the Innovative Fusion Technologies of Intelligent Antenna Material/Structure/Network for THz 6G, 50%; in part by the Samsung Electronics (Development of Dualband/Wide-band High Efficiency Power Amplifier MMIC for 5G Applications, 50%); and in part by the Chip Fabrication and EDA Tool through the IC Design Education Center (IDEC), South Korea. (Corresponding author: Jungsuek Oh.)

The authors are with the Department of Electrical and Computer Engineering (ECE), Institute of New Media and Communications (INMC), Seoul National University, Seoul 151-742, South Korea (e-mail: jungsuek@snu.ac.kr).

Color versions of one or more figures in this letter are available at <https://doi.org/10.1109/LMWT.2023.3270660>.

Digital Object Identifier 10.1109/LMWT.2023.3270660

2771-957X © 2023 IEEE. Personal use is permitted, but republication/redistribution requires IEEE permission. See <https://www.ieee.org/publications/rights/index.html> for more information.

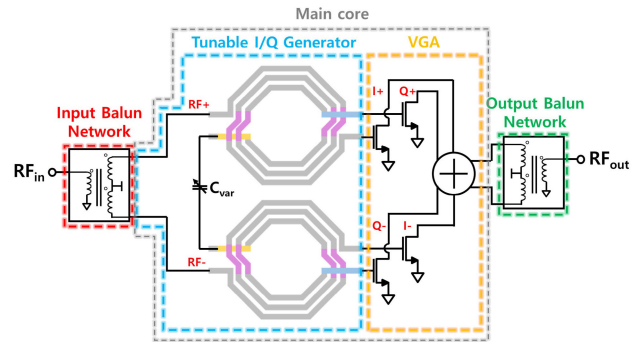


Fig. 1. Schematic of the proposed vector modulator and tunable I/Q generator.

reflection phase shifters [5], switched line phase shifters [6], [7], and active type, vector modulators [8], [9], [10]. Owing to the advantage of being able to control a continuous phase shift with a high gain, the demand for vector modulators has significantly increased. The bottleneck of the vector modulator is that the I/Q generator has a high loss and low bandwidth. To overcome I/Q generator issues, an embedded I/Q generator has been proposed beyond all-pass filters or an *RC* polyphase filter (PPF), and these techniques can increase the gain or phase resolution [11], [12], [13]. However, the coupler design without tuning operation along with the frequency is applied, so, their bandwidth and phase error are still limited.

To address the aforementioned issues, a tunable I/Q generator was proposed based on a transformer-based coupler to achieve compact size and high gain, and frequency selection was possible by varactor control. Based on the proposed I/Q generator, a low phase error with a high-gain vector modulator was demonstrated in this study.

## II. CIRCUIT DESIGN

A block diagram of the proposed vector modulator is demonstrated in Fig. 1. The input signal flows to the input balun network (IBN) and is converted into a differential signal. Then, the signal is split into a quadrature signal by the I/Q generator. The variable gain amplifier (VGA) amplifies the quadrature signal along with bias control, and the amplified signal is combined in the output balun network (OBN).

As shown in Fig. 2(a), the IBN comprises an *LC* matching network, a transformer to implement the balun, and cascode amplifier. The cascode amplifier is optimized to maximize the gain of the vector modulator. Even if the VGA in the main core can amplify the signal, the input impedance of the main

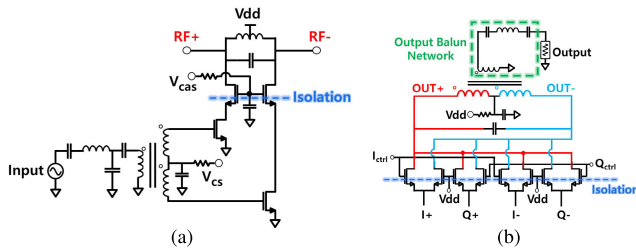


Fig. 2. Schematic of the proposed vector modulator. (a) IBN. (b) VGA with OBN.

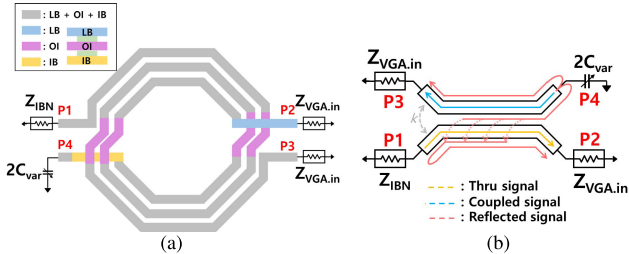


Fig. 3. Single part of the proposed tunable I/Q generator. (a) Layout of the proposed asymmetric load coupler. (b) Simplified operation diagram of the proposed coupler.

core is focused on minimizing the quadrature signal error. Due to this reason, the transistor is optimized to increase the gain of the circuit. In addition, the output impedance of the IBN is used to generate the quadrature signal. Therefore, the high isolation between the IBN and the I/Q generator should be designed to maintain constant phase differences, irrespective of the VGA operation. A cascode amplifier is used to achieve isolation and high gain in the IBN design by implementing ac ground on the transistor gate.

The main core consists of a VGA and tunable I/Q generator proposed in two transformer-based couplers and a varactor topology. Fig. 3(a) shows the diagram of a single part of the tunable I/Q generator. A three-metal stacked layer is used to design the coupler to increase the coupling coefficient and minimize its size. As shown in Fig. 3(b), the drain impedance of the IBN transistor is loaded to the input port, P1, whereas the thru and coupled ports, P2 and P3, are attached to the current source gate of the VGA, and the isolation port, P4, is connected to the varactor. A differential signal is applied to P1 of each coupler, and P4 is separated from the virtual ground. Because asymmetric impedances are loaded into the proposed coupler on each port, signal cancellation cannot occur at P4. Thus, multiple reflections are produced in the coupler, and the reflected signal is transmitted to other ports by coupling. The amount of reflection changes along the capacitance of the varactor; therefore, the phase and magnitude of the thru and coupled signals can be controlled by the varactor voltage. Furthermore, the coupling coefficient of the coupler,  $k$ , is 0.6. Therefore, multireflection is considered up to two times for the tunable I/Q generation design, as shown in Fig. 3(b).

Fig. 4(a) shows the phase and magnitude difference between P2 and P3 along the varactor control when the impedance is loaded on each coupler port as shown in Fig. 3(b). The phase and magnitude difference of the thru and coupled signals are approximately 0 dB and  $90^\circ$ , respectively, are formed in a single frequency, and the frequency is adjusted by the varactor

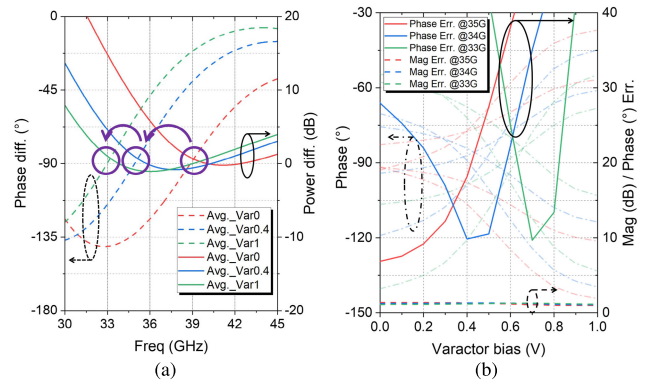


Fig. 4. Phase and magnitude difference graph of the proposed tunable I/Q generator. (a) Phase and magnitude difference of the proposed I/Q generator without the VGA core. (b) Signal phase and magnitude difference of the proposed I/Q generator with the VGA core.

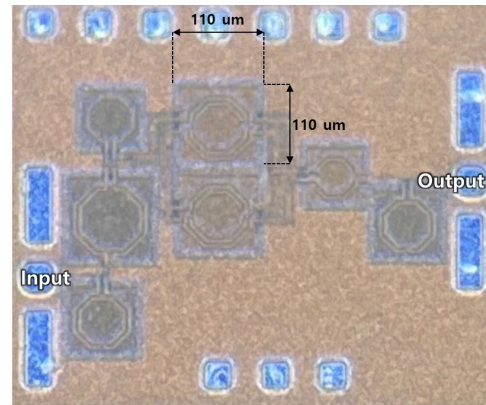


Fig. 5. Photograph of the proposed vector modulator.

bias voltage from 0 to 1 V. Therefore, the asymmetric load coupler generates the I/Q signal and implements a wide tuning range with the minimization of the phase and magnitude difference. Fig. 4(b) shows the variation in the coupler signal with the VGA. It is elaborated that the quadrature signal phase can be varied by changing the varactor voltage and the signals are represented in dash-dotted line on the left axis. The magnitude error is suppressed below 1 dB, irrespective of the varactor variation presented on the right axis. Moreover, the phase error can be maintained below  $10^\circ$  with a constant magnitude error even if the frequency is changed. Therefore, the proposed I/Q generator achieves frequency-optimized operation.

A schematic of the VGA core and OBN is shown in Fig. 2(b). The VGA core utilizes the Gilbert cell topology. The Gilbert cell topology also helps increase the vector modulator's gain, but the VGA should be more targeted to generate the quadrature signal. Therefore, the transistors utilized in the VGA are optimized to minimize the amplitude and phase loss of the I/Q signal rather than the gain. Moreover, a large capacitor is connected to the gate of the common gate transistor; therefore, high isolation between the VGA and OBN can be achieved. The OBN consists of a transformer to convert the differential signal into a single-ended signal and an additional LC matching network to obtain wideband characteristics.

### III. MEASUREMENT RESULTS

The proposed vector modulator was fabricated in a 28 nm CMOS process with a circuit area of  $820 \times 500 \mu\text{m}$ , and a

TABLE I  
PERFORMANCE SUMMARY AND COMPARISON RESULTS OF VECTOR MODULATOR

Reference	This work	RFIC [4]	JSSC [5]	TCAS II [6]	MWCL [7]	RFIC [8]
Frequency (GHz)	31-36	26-28	78.8-92.8	24-28	52-57	32-40
Technology	28nm CMOS	130nm SiGe	28nm CMOS	65nm CMOS	40nm CMOS	65nm CMOS
Type	ALTTC*	2 Stage RC PPF	lumped-element quadrature coupler	Transformer-based digital-tunable QAF	Hybrid (Passive + Active)	Passive-type
Phase res.	4-bit	5-bit	4-bit	6-bit	6-bit	7-bit
RMS Phase Err. at $f_0$ (°)	1.93	4	9.4	1.4	2.8-3.76	0.45**
RMS Gain Err. at $f_0$ (dB)	1.11	0.2	1.68	0.25	2.07-2.23	0.17**
Avg Gain. at $f_0$ (dB)	-3.48	-0.5	2.3	-7.4	-14**	-16.9**
Pdc (mW)	28.8	23	21.6	31.9	14.3	0

\* Asymmetric-loaded tunable transformer-based coupler

\*\* Graphically estimated from the reported figures

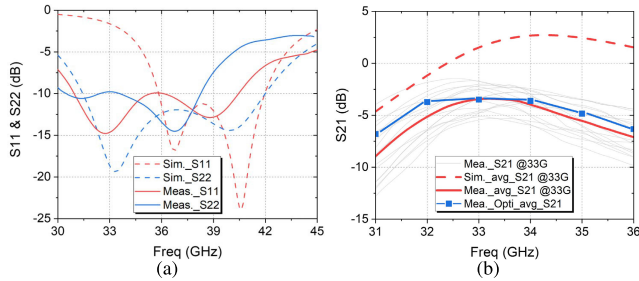


Fig. 6. Simulation and measurement  $S$ -parameter results of the proposed tunable I/Q generator. (a)  $S_{11}$  and  $S_{22}$  simulation and measurement results. (b)  $S_{21}$  magnitude results along the varactor operation.

photograph of the chip is shown in Fig. 5. Additionally, the power consumption of the vector modulator was 28.8 mW from a 1.8 V supply voltage.

Fig. 6 shows the simulation and measurement  $S$ -parameter results. The proposed vector modulator was implemented in high isolation between the IBN, main core, and OBN; therefore,  $S_{11}$  and  $S_{22}$  had constant values irrespective of VGA operation. Based on the  $S_{11}$  and  $S_{22}$  values, the  $-10$  dB bandwidth of the vector modulator was measured as 7 GHz.  $S_{21}$  comparison results are shown in Fig. 6(b). When the varactor bias was optimized to 33 GHz, the magnitude of  $S_{21}$  was maximized, and the value decreased with frequency variation. Otherwise, when the varactor bias was adjusted to the target frequency, the average  $S_{21}$  value increased. Therefore, the 3 dB bandwidth of the proposed vector modulator operation was approximately 5 GHz, from 31 to 36 GHz. The measurement results of the phase shift operation are shown in Fig. 7(a). The phase was shifted within  $22.5^\circ$ , resulting in a root-mean-square (rms) error of approximately  $2^\circ$  at a target frequency of 33 GHz. The detailed rms phase and magnitude errors are shown in Fig. 7(b). As shown in Fig. 7(b), the rms magnitude error was almost constant and was lower than 2 dB, irrespective of the varactor tuning. However, the rms phase error significantly increased to  $11.55^\circ$  at 36 GHz without varactor operation. By changing the varactor bias from 0 to 1.05 V, the operation frequency of the I/Q generator could be adjusted, and the rms phase error could be maintained below  $5^\circ$  within the proposed vector modulator bandwidth. This could represent a phase error minimization of approximately  $3^\circ$  by tuning the I/Q generator. Table I presents a summary of the performance

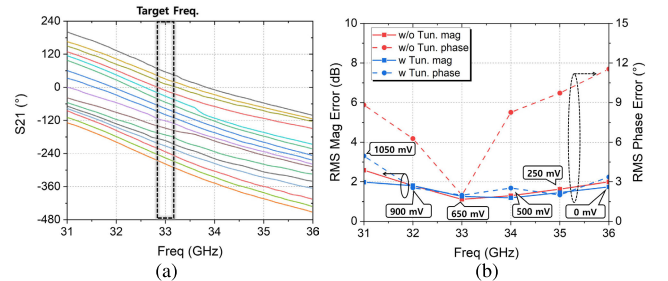


Fig. 7. Measurement  $S_{21}$  phase results of the vector modulator. (a)  $S_{21}$  phase graph in which the varactor is optimized at 33 GHz. (b) rms phase and magnitude error along with the varactor operation.

of the measured vector modulator and its comparison with other state-of-the-art technologies. The proposed vector modulator based on the tunable I/Q generator achieved a low phase error with a high gain over a wide frequency range.

#### IV. CONCLUSION

This study proposed a high-performance vector modulator with a tunable I/Q generator. The vector modulator comprised a wideband IBN, an OBN with an  $LC$  matching network, I/Q generator, and a VGA core. The tunable I/Q generator was implemented with a low phase error of the quadrature signal by combining two transformer-based couplers and one varactor. The coupler was connected to asymmetric loads; thus, multiple reflections were generated, and the reflection signal was controlled by the varactor. Therefore, the quadrature signals could be maintained at a  $90^\circ$  phase difference along with frequency variation. Based on the tunable I/Q generator, a 4-bit low phase rms error vector modulator was designed. In the 31–36 GHz range, the rms phase error was  $1.98^\circ$ – $4.95^\circ$ . The rms gain error and an average peak gain were 1.11 and  $-3.48$  dB, respectively, at 33 GHz. The proposed vector modulator had the advantages of a high gain and low phase error in the bandwidth by adjusting the target frequency. Therefore, this is a good candidate for 5G mmWave communication systems.

#### REFERENCES

- [1] W. Zhu et al., "A 24–28-GHz four-element phased-array transceiver front end with 21.1%/16.6% transmitter peak/OP1dB PAE and sub-degree phase resolution supporting 2.4 Gb/s in 256-QAM for 5-G communications," *IEEE Trans. Microw. Theory Techn.*, vol. 69, no. 6, pp. 2854–2869, Jun. 2021.

- [2] S. R. Boroujeni et al., "A high-efficiency 27–30-GHz 130-nm bi-CMOS transmitter front end for SATCOM phased arrays," *IEEE Trans. Microw. Theory Techn.*, vol. 69, no. 11, pp. 4977–4985, Nov. 2021.
- [3] L. Gao and G. M. Rebeiz, "A 22–44-GHz phased-array receive beamformer in 45-nm CMOS SOI for 5G applications with 3–3.6-dB NF," *IEEE Trans. Microw. Theory Techn.*, vol. 68, no. 11, pp. 4765–4774, Nov. 2020.
- [4] B.-W. Min and G. M. Rebeiz, "Single-ended and differential Ka-band BiCMOS phased array front-ends," *IEEE J. Solid-State Circuits*, vol. 43, no. 10, pp. 2239–2250, Oct. 2008.
- [5] X. Li, B. Liu, H. Fu, and K. Ma, "A 30–36 GHz passive hybrid phase shifter with a transformer-based high-resolution reflect-type phase shifting technique," *IEEE Trans. Circuits Syst. II, Exp. Briefs*, vol. 68, no. 7, pp. 2419–2423, Jul. 2021.
- [6] G. S. Shin et al., "Low insertion loss, compact 4-bit phase shifter in 65 nm CMOS for 5G applications," *IEEE Microw. Wireless Compon. Lett.*, vol. 26, no. 1, pp. 37–39, Jan. 2016.
- [7] J.-H. Tsai, Y.-L. Tung, and Y.-H. Lin, "A 27–42-GHz low phase error 5-bit passive phase shifter in 65-nm CMOS technology," *IEEE Microw. Wireless Compon. Lett.*, vol. 30, no. 9, pp. 900–903, Sep. 2020.
- [8] J. Xia and S. Boumaiza, "Digitally assisted 28 GHz active phase shifter with 0.1 dB/0.5° RMS magnitude/phase errors and enhanced linearity," *IEEE Trans. Circuits Syst. II, Exp. Briefs*, vol. 66, no. 6, pp. 914–918, Jun. 2019.
- [9] Y. Li et al., "A 32–40 GHz 7-bit CMOS phase shifter with 0.38 dB/1.6° RMS magnitude/phase errors for phased array systems," in *Proc. IEEE Radio Freq. Integr. Circuits Symp. (RFIC)*, Nagoya, Japan, Aug. 2020, pp. 319–322.
- [10] D. Pepe and D. Zito, "Two mm-wave vector modulator active phase shifters with novel IQ generator in 28 nm FDSOI CMOS," *IEEE J. Solid-State Circuits*, vol. 52, no. 2, pp. 344–356, Feb. 2017.
- [11] N. Wei et al., "A calibration scheme for 24–28-GHz variable-gain phase shifter in 65-nm CMOS," *IEEE Trans. Circuits Syst. II, Exp. Briefs*, vol. 69, no. 4, pp. 1996–2000, Apr. 2022.
- [12] X. Quan, "A 52–57 GHz 6-bit phase shifter with hybrid of passive and active structures," *IEEE Microw. Wireless Compon. Lett.*, vol. 28, no. 3, pp. 236–238, Mar. 2018.
- [13] S. P. Sah and D. Heo, "An ultra-wideband 15–35 GHz phase-shifter for beamforming applications," in *Proc. Eur. Microw. Integr. Circuit Conf. (EuMIC)*, Apr. 2013, pp. 264–267.